Volume 49
Number 13
7 April 2025
Pages 5153–5604

NJC

New Journal of Chemistry

A journal for new directions in chemistry

rsc.li/njc

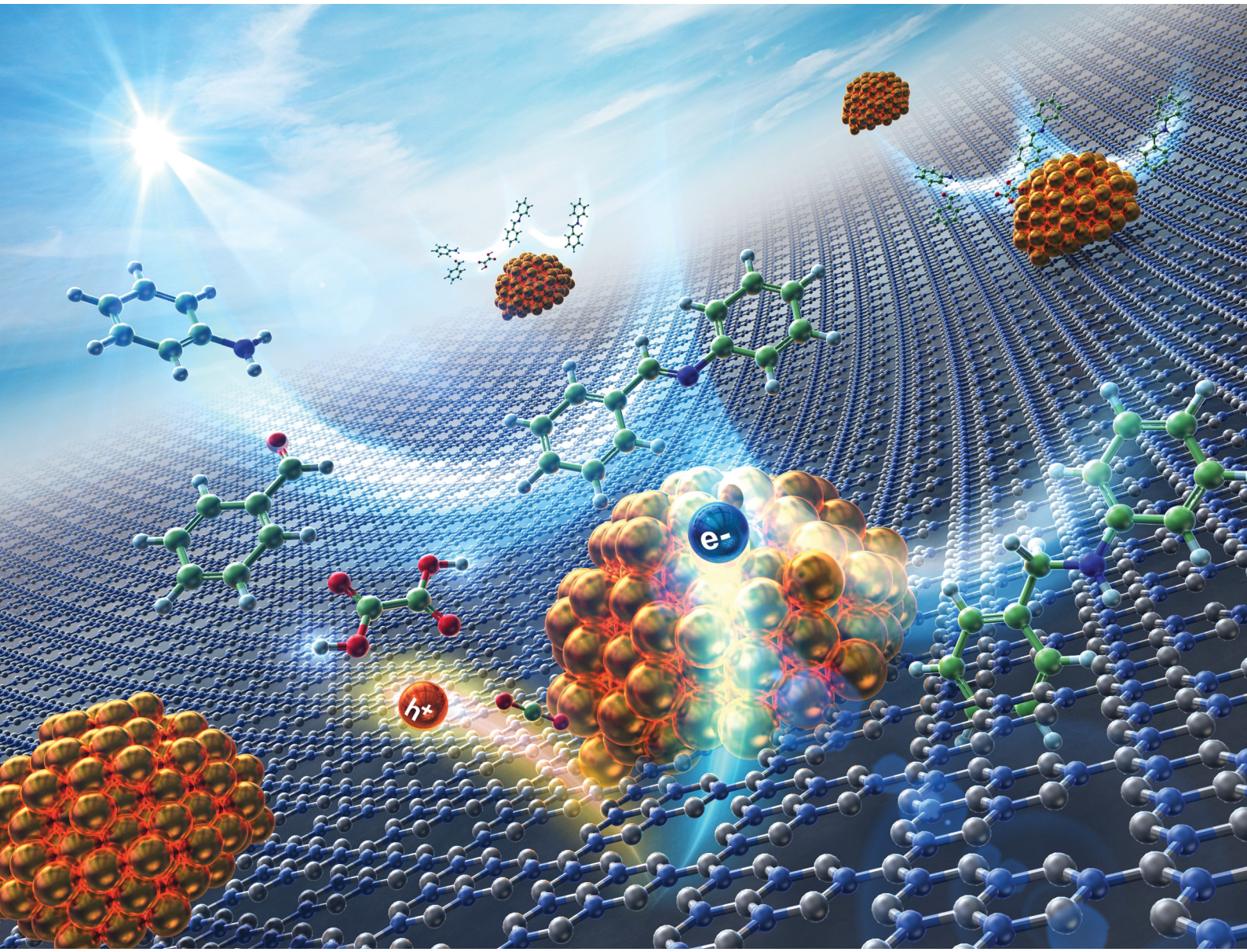

ISSN 1144-0546

PAPER

Hiroshi Kominami *et al.*

Bi-functionality of organic acids as acid catalysts and a hydrogen source for one-pot production of secondary amines from primary amines and aromatic aldehydes over an Au–C_3N_4 photocatalyst

ROYAL SOCIETY OF CHEMISTRY

cnrs

NJC

ROYAL SOCIETY OF CHEMISTRY

PAPER

View Article Online
View Journal | View Issue

Cite this: *New J. Chem.*, 2025, 49, 5167

Bi-functionality of organic acids as acid catalysts and a hydrogen source for one-pot production of secondary amines from primary amines and aromatic aldehydes over an Au–C_3N_4 photocatalyst†

Hiroshi Kominami, *[a] Xiangru Liu[b] and Atsuhiro Tanaka [a]

Carbon nitride modified with a gold (Au) cocatalyst (Au–C_3N_4) was utilized in a one-pot synthesis of *N*-phenylbenzylamine (PBA) from benzaldehyde (BAD) and aniline (AN) in the presence of an organic acid. In this process, the organic acid fulfilled two functions: (1) as an acid catalyst for the condensation of AN and BAD, producing benzylideneaniline (BAN) in the initial thermal step, and (2) as a hole scavenger (hydrogen source) for the hydrogenation of BAN to PBA in the subsequent photocatalytic step over Au–C_3N_4. Various organic acids were utilized, and oxalic acid was found to be the most effective due to its capacity to maintain an acidic pH environment as a divalent acid and its ability to effectively capture positive holes as a hole scavenger, resulting in the generation of carbon dioxide. Photoirradiation of the system under equilibrium conditions in the condensation process induced effective hydrogenation of BAN, resulting in the production of PBA with a yield of >99%. A series of experiments were conducted to study the action spectrum, the impact of alcohols, and reusability, and halogen-substituted PBA was synthesized. The outcomes of this study demonstrate the efficacy of oxalic acid in photocatalytic reactions and the potential of a cocatalyst-loaded C_3N_4 photocatalyst for organic synthesis.

Received 27th December 2024,
Accepted 23rd February 2025

DOI: 10.1039/d4nj05500d

rsc.li/njc

1. Introduction

Amine compounds are important in the field of organic chemistry with a wide range of applications including applications in pharmaceuticals, agrochemicals, and cosmetics.[1,2] Consequently, extensive research on the synthesis of amine compounds has been conducted. However, in industrial production, there are considerable challenges associated with the generation of by-products, high toxicity of waste products, and high cost of synthesis. There are particular concerns about the environmental and operational hazards associated with traditional secondary amine synthesis methods. In such processes, there are concerns about the generation of toxic by-products, utilization of hazardous materials including high-pressure hydrogen gas and strong bases, consumption of valuable resources, necessity for precious metal catalysts, and the energy-consuming nature of certain synthetic procedures.[3–6] Furthermore, the treatment and disposal of waste materials containing heavy metals and undesirable organic solvents necessitate the implementation of specific and often costly handling procedures to mitigate their environmental impact. Consequently, there has been a notable increase in interest shown in photocatalytic synthesis of secondary amines.[7–9]

Recently, hydrogen-free one-pot synthesis of *N*-phenylbenzylamine (PBA) from benzaldehyde (BAD) and aniline (AN) over an Au–TiO_2 photocatalyst has been reported.[10] This process consists of two steps: (1) formation of benzylideneaniline (BAN) and water by condensation of AN and BAD, which is an acid-catalyzed thermal reaction, and (2) photocatalytic hydrogenation of BAN to PBA through a hydrogen transfer reaction from alcohol. This has led to increased interest in the same reaction using other photocatalysts.

Carbon nitride (C_3N_4), a conjugated polymer with a graphite-like structure, has emerged as a new research area of interest in the fields of artificial photosynthesis and environmental restoration as a metal-free, visible light-responsive photocatalyst.[11,12] Its high chemical stability, low cost, lack of depletion concerns, and its energy band structure (E_g = 2.6 eV), which enables it to utilize visible light, are of particular interest. However, limited catalytic

[a] *Department of Applied Chemistry, Faculty of Science and Engineering, Kindai University, 3-4-1, Kowakae, Higashiosaka, Osaka 577-8502, Japan. E-mail: hiro@apch.kindai.ac.jp*
[b] *Department of Molecular and Material Engineering, Graduate School of Science and Engineering, Kindai University, 3-4-1, Kowakae, Higashiosaka, Osaka 577-8502, Japan*

† Electronic supplementary information (ESI) available. See DOI: https://doi.org/10.1039/d4nj05500d

activity due to low conductivity and small specific surface area has limited the applications of C_3N_4. Methods to enhance the photocatalytic activity of C_3N_4 include modifications of the molecular structure and the formation of complexes with other semiconductors.[13–16] Modification of the molecular structure results in alterations of the distinctive π–π conjugated electronic structure of C_3N_4, thereby reducing the probability of recombination of excited electrons and holes. Modifying the ratio of nitrogen to carbon in C_3N_4 also affects the band gap energy, thereby widening the wavelength range of light that can be absorbed by the photocatalyst and enhancing the efficiency of electron excitation. It has been demonstrated that the introduction of a cocatalyst to a photocatalyst can expand the range of its applications. This is due to the fact that the reducing property of the photocatalyst can be controlled by the cocatalyst. As a result, there may be various applications of C_3N_4 in organic synthesis when an appropriate cocatalyst is selected for the desired reaction.

In this study, we found that an Au–C_3N_4 photocatalyst can be successfully used for one-pot synthesis of secondary amines from primary amines and aldehydes. In contrast to the TiO_2 system, an acid compound is required for the initial step because C_3N_4 does not function as an acid catalyst. Given that organic acids possess bi-functions (an acid and a hydrogen source) that are essential for

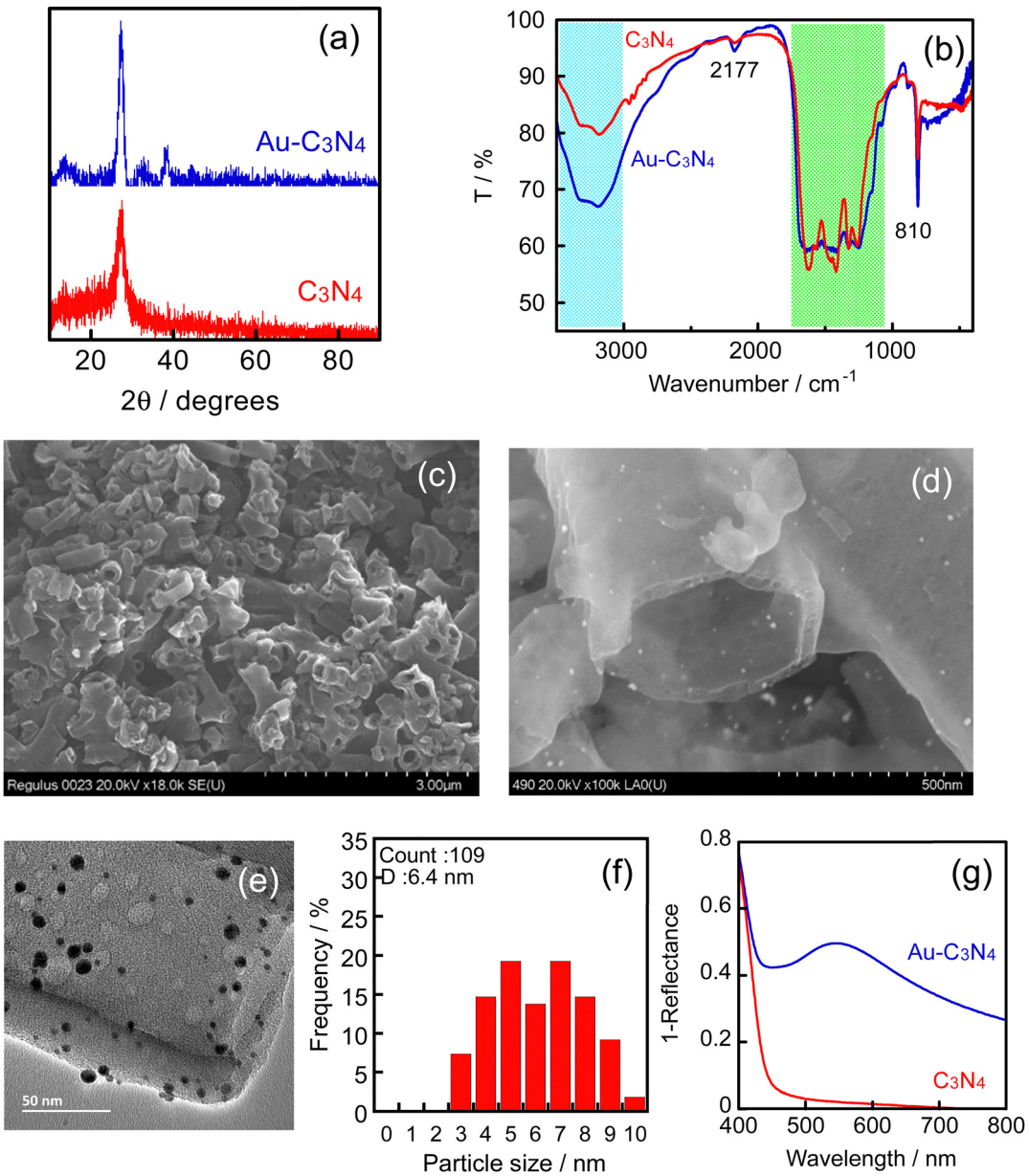

Fig. 1 (a) XRD patterns of C_3N_4 and 1 wt% Au–C_3N_4, (b) FT-IR spectrum of C_3N_4 and 1 wt% Au–C_3N_4, (c) SEM photograph of C_3N_4, (d) SEM photograph of 1 wt% Au–C_3N_4, (e) TEM photograph of 1 wt% Au–C_3N_4, (f) size distribution of Au nanoparticles loaded on C_3N_4, and (g) photoabsorption spectra of C_3N_4 and 1 wt% Au–C_3N_4.

this reaction, an examination of them within the Au–C_3N_4 system was carried out. This approach addresses the environmental and safety concerns associated with traditional synthetic methods by minimizing the use of hazardous materials, reducing energy consumption, and reducing the formation of toxic byproducts. Consequently, this method emerges as a more environmentally friendly alternative for the production of secondary amines and demonstrates the potential of a cocatalyst-loaded C_3N_4 photocatalyst for organic synthesis.

2. Experimental

All experimental procedures (chemicals, preparation and characterization of samples, and photocatalytic reactions) are provided in the ESI.†

3. Results and discussion

3.1 Characterization of C_3N_4 and Au–C_3N_4

The specific surface area of the C_3N_4 sample was calculated to be 36 $m^2\ g^{-1}$. The XRD pattern of C_3N_4 exhibited two diffraction peaks at 2θ = 12.7° and 27.4°, corresponding to the (100) and (002) crystal planes of C_3N_4, respectively (Fig. 1(a)). In the XRD pattern of Au–C_3N_4, a weak peak was observed at 38.3°, indicative of the (111) diffraction peak of Au. In the FTIR spectrum of C_3N_4, characteristic peaks indicative of tri-*s*-triazine at 810 cm^{-1}, C–N heterocycles at 1200–1700 cm^{-1}, –C≡N at 2177 cm^{-1}, and H_2O and $-NH_x$ at 3000–3500 cm^{-1} were observed (Fig. 1(b)), thereby indicating that the sample prepared by the present method possesses the characteristic C_3N_4 structure. In the spectrum of Au–C_3N_4, the peaks attributable to C–N heterocycles appear to have been weakened, suggesting that the structure has been slightly affected by photodeposition of the Au cocatalyst. SEM observation revealed that C_3N_4 prepared by the present method was composed of a tubular structure with an average diameter of *ca.* 300 nm (Fig. 1(c)). The atomic ratio of carbon and nitrogen was determined to be 3.0 : 4.3 by means of an energy dispersive X-ray spectroscopy unit attached to a scanning electron microscope. Fine particles of Au were observed in the SEM photograph (Fig. 1(d)). TEM analysis of Au–C_3N_4 revealed the presence of defects in the wall of the C_3N_4 tube, with Au particles dispersed on the wall (Fig. 1(e)). The average diameter of the Au particles was determined to be 6.4 nm, exhibiting a relatively wide distribution (Fig. 1(f)). The absorption spectra of C_3N_4 and Au–C_3N_4 are shown in Fig. 1(g). The spectrum of C_3N_4 exhibited photoabsorption in the visible light region, while the spectrum of Au–C_3N_4 demonstrated a substantial enhancement in photoabsorption within the visible light region, attributed to surface plasmon resonance and light scattering of the Au particles.

3.2. Effects of organic acids on formation of imine by condensation of aldehyde and amine in the dark

Since formation of BAN by condensation of AN and BAD (Scheme 1) is not a photocatalytic process but a homogeneous thermal reaction, this reaction was examined under various conditions in the dark.[17–21]

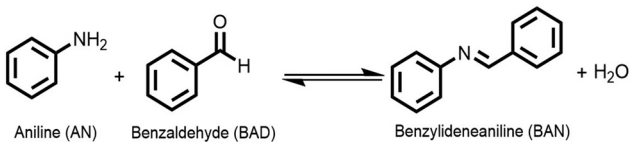

Scheme 1 Thermal condensation of AN and BAN to BAN and water (equilibrium reaction).

Condensation of AN and BAD in 2-propanol was very slow (Fig. 2(a)) and Au–C_3N_4 showed only a small effect on condensation in the dark (Fig. 2(b)). In the case of production of BAN from AN and BAD, Au–TiO_2 played a significant role in the first process as an acid catalyst.[10] The small rate of condensation of AN and BAD in the presence of Au–C_3N_4 is due to the weak (or no) acidity of C_3N_4, indicating that an acid compound is necessary to promote the production of BAN and the subsequent hydrogenation of BAN. For rapid production of BAN, oxalic acid (OA) was added to 2-propanol solutions of AN and BAD in the absence and presence of Au–C_3N_4. As expected, OA accelerated the condensation of AN and BAD, and the production of BAN reached an equilibrium within 30 min (Fig. 2(c)) with the presence of Au–C_3N_4 having no effect (Fig. 2(d)). Some organic acids were also examined, and the results are shown in Table 1. Among the organic acids examined, OA and citric acid were effective for production of BAN. When these acids were added to the reaction mixture, the values of pH greatly decreased, indicating that a large number of protons provided by the acids accelerated the condensation of AN and BAD.

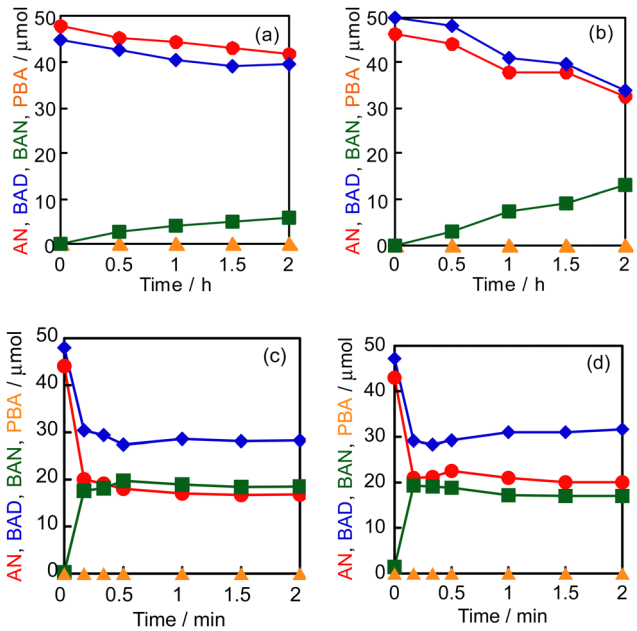

Fig. 2 Production of BAN (■) by condensation of AN (●) and BAD (◆) in 2-propanol suspensions under various conditions: (a) with no additive, (b) in the presence of 1 wt% Au–C_3N_4 (50 mg), (c) in the presence of OA (100 μmol), and (d) in the presence of OA (100 μmol) and 1 wt% Au–C_3N_4 (50 mg). PBA (▲) was not produced in all cases.

Table 1 Production of BAN by condensation of AN and BAD in 2-propanol suspensions of 1 wt%Au–C_3N_4 in the presence of organic acids in the dark[a]

Entry	Organic acid[b]	pH[c]	BAN formation/μmol
1	Formic acid	4.54	18.1
2	Oxalic acid	2.22	20.0
3	Benzoic acid	4.61	18.0
4	Citric acid	2.92	22.9

[a] Reaction time: 0.5 h. [b] 100 μmol. [c] pH of suspension.

3.3. Production of secondary amine by photocatalytic hydrogenation of imine

After the condensation of AN and BAD to BAN reached an equilibrium, the 2-propanol suspension containing AN, BAD, BAN, OA and Au–C_3N_4 was photoirradiated. The time courses of the amounts of these compounds and H_2 and CO_2 are shown in Fig. 3. Just after photoirradiation of the suspension, PBA was produced and the amount increased linearly, indicating that hydrogenation of BAN occurred in the reaction mixture. To maintain the equilibrium in the condensation reaction, AN and BAD were continuously consumed. The amount of BAN also gradually decreased, indicating that the photocatalytic hydrogenation of BAN to PBA efficiently occurred over Au–C_3N_4 under the present conditions. The yield of PBA reached >99% after photoirradiation for 5.5 h. CO_2 was produced as the oxidized product of OA. The overall reaction of the hydrogenation of BAN to PBA is shown in Scheme 2. In this step, the C=N bond of BAN is hydrogenated by active hydrogen species over an Au cocatalyst. Active hydrogen species are produced from photogenerated electrons and protons provided by organic acids.

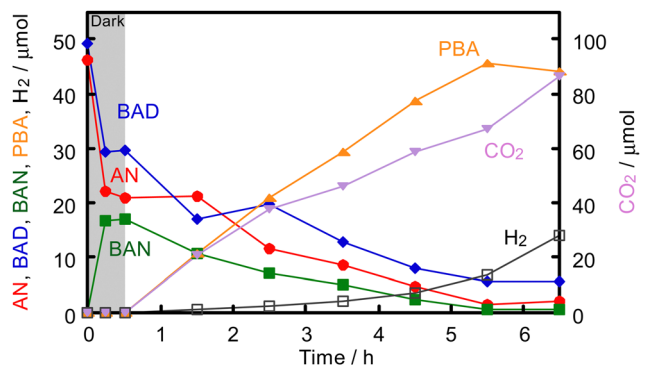

Fig. 3 Time courses of the amounts of BAD (◆), AN (●), BAN (■), PBA (▲), CO_2 (▼) and H_2 (□) in a 2-propanol suspension of Au–C_3N_4 in the presence of OA as an acid catalyst and a hole scavenger. The reaction was carried out in the dark for the first 0.5 h and under irradiation of UV light from a mercury lamp from 0.5 to 6.5 h.

$$(COOH)_2 \rightarrow H_2 + 2CO_2$$

Scheme 3 Photocatalytic production of H_2 from OA.

H_2 was observed at around the last stage of hydrogenation, indicating that the reduction of protons ($2H^+ + 2e^- \rightarrow H_2$) also occurred. The production of H_2 is shown in Scheme 3.

CO_2 was produced as the oxidized product with progress of the formation of PBA and H_2. From the stoichiometry of the reaction (Scheme 2), the ideal ratio of PBA and CO_2 produced is 2. According to Scheme 3, the ratio of H_2 and CO_2 produced is also 2. From the yields of PBA (45 μmol) and H_2 (10 μmol) at 5.5 h, the amounts of OA consumed for these productions and the yield of CO_2 were expected to be 55 μmol and 110 μmol, respectively. The amount of CO_2 observed in the gas phase was *ca.* 90 μmol, which was slightly smaller than the expected value. One probable explanation for this phenomenon is that the solvent 2-propanol also functioned as a hole scavenger and underwent oxidation to acetone, thereby saving the consumption of OA and reducing the CO_2 production.

We also examined the effects of different amounts of OA on the yield of PBA, and the results are shown in Fig. S1 (ESI†). When the amount of OA was reduced to 50 μmol, the yield of PBA at 3.5 h (= 0.5 h + 3 h) decreased. The amount of OA is the stoichiometric amount required for the photocatalytic hydrogenation of BAN to PBA. In the photocatalytic hydrogenation of BAN consuming OA as the hole scavenger (Scheme 2), OA is still necessary as the acid catalyst for condensation of AN and BAD remaining in the reaction mixture (Scheme 1). Therefore, a slight excess of OA is required to maintain a continuous rate in the condensation reaction and the amount was 50% (25 μmol) as Fig. S1 (ESI†) shows. A further increase in the amount of OA showed no positive or negative effect on the production of PBA.

An action spectrum was obtained to confirm that the hydrogenation of BAN was induced by photoabsorption of C_3N_4. The action spectrum of PBA production is also shown in Fig. 4. The value of AQE increased with decrease in the wavelength of light (increase in photon energy) and reached 2.5% at 400 nm. It was observed that there is a considerable difference between AQE and photoabsorption of C_3N_4 at 420 nm, indicating that the photoabsorption of C_3N_4 at around 420 nm does not significantly contribute to the hydrogenation of BAN.

In order to evaluate the presence of H_2 in the gas phase, a dark reaction was carried out in a 2-propanol suspension containing AN, BAD, BAN, OA, and Au–C_3N_4 under 1 atm H_2 (see Fig. S2, ESI†). Upon attaining the equilibrium of condensation of AN and BAD, a discernible alteration in the composition of the liquid phase was not observed, thereby suggesting that

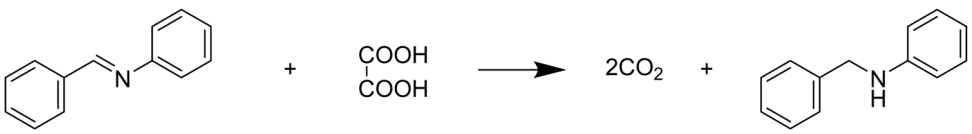

Scheme 2 Photocatalytic reaction of BAN and OA to PBA and CO_2.

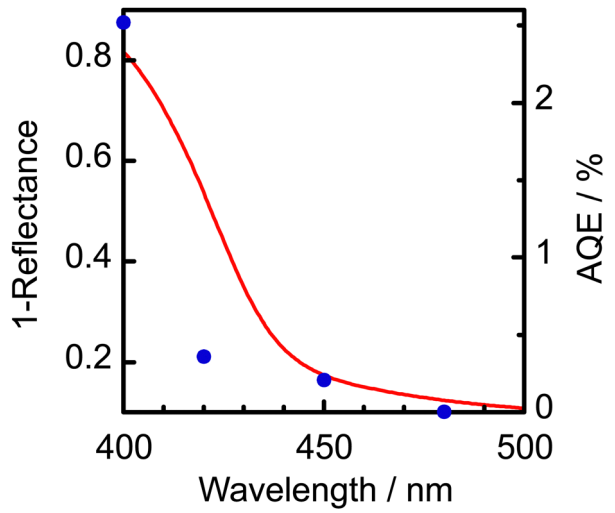

Fig. 4 An action spectrum of PBA production over Au–C_3N_4.

H_2 in the gas phase did not contribute to the hydrogenation of BAN.

The duration of the usability of the Au–C_3N_4 photocatalyst was evaluated. After the photocatalytic hydrogenation of BAN under light irradiation for 5 h, the Au–C_3N_4 photocatalyst was separated from the reaction mixture by filtration, washed with distilled water, and dried at 80 °C for 12 h *in vacuo*. The recovered Au–C_3N_4 photocatalyst was used again for condensation in the dark for 1 h and hydrogenation under light irradiation for 5 h. The same procedure was repeated and the Au–C_3N_4 photocatalyst was used for the reaction (Fig. S3, ESI†). PBA was produced almost quantitatively, indicating that Au–C_3N_4 can be used at least three times without losing catalytic performance.

Fig. 5(a) shows effects of organic acids (100 μmol) on the production of PBA from AN and BAD *via* BAN in 2-propanol suspensions of Au–C_3N_4 in the dark reaction for 0.5 h and subsequent photocatalytic reaction for 2 h. The largest yield of PBA was obtained when OA was used. It is expected that efficient hole trapping by OA occurs because OA is directly converted to CO_2 and then CO_2 is removed from the surface of C_3N_4. The same explanation can be applied to a relatively large yield of PBA in the case of formic acid. In the case of citric acid, the yield of PBA was small probably due to adsorption of the intermediate(s) produced by the oxidation of citric acid, although citric acid was effective for the condensation of BAD and AN as shown in Table 1. When benzoic acid was used as a hole scavenger, the yield of PBA was small probably due to the adsorption of the intermediate(s) produced by the oxidation of benzoic acid.

Table 2 Reactions of chlorine-substituted ANs and BADs in 2-propanol suspensions of Au–C_3N_4 in the presence of OA before and after light irradiation[a]

Entry	Substrates		Yield/%	
	ANs	BADs	PBA	Cl-PBA
1			>99	—
2		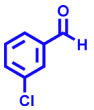	<1	56
3			<1	70
4		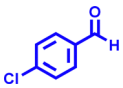	<1	76
5			0	86
6	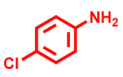		17	63

[a] ANs: 45 μmol, BADs: 50 μmol, OA: 100 μmol, 2-propanol: 5 cm^3, Au–C_3N_4: 50 mg, time for condensation in the dark: 0.5 h, and time for photocatalytic reaction under light irradiation: 5 h.

Fig. 5(b) shows the effects of solvent alcohols on the production of PBA from AN and BAD *via* the production of BAN in a suspension of Au–C_3N_4 in the presence of OA (100 μmol) in the dark reaction for 0.5 h and subsequent photocatalytic reaction for 2 h. All alcohols can be used, and the largest PBA yield was obtained when methanol was used. This finding suggests that solvents with greater polarity show enhanced performance.

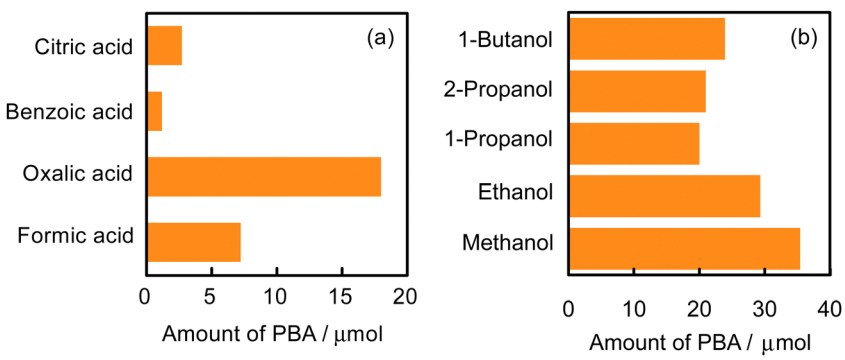

Fig. 5 Effects of (a) organic acid (100 μmol) in 2-propanol and (b) alcohol solvents containing OA (100 μmol) on production of PBA from AN and BAD *via* BAN in the suspension of 1 wt% Au–C_3N_4 in the dark for 0.5 h and under subsequent light irradiation for 2 h.

Water would be the optimal solvent for this reaction due to its greater polarity than that of methanol. However, this was not the case because the equilibrium of condensation was shifted to the reverse side in the presence of water. Acetonitrile is a potential candidate for use as a solvent in this reaction. However, the decision to utilize alcohols as the solvent was made on the basis of their superior environmental compatibility in comparison to acetonitrile.

We applied 1 wt% Au–C_3N_4 to produce chlorine-substituted PBA (Cl-PBAs) under the same conditions as those for unsubstituted AN and BAD. The introduction of another functional group can be achieved through the substitution of the chlorine group, as it is a highly effective leaving group. Consequently, during the hydrogenation process (second step), the chlorine group is frequently lost from the benzene ring. Therefore, the production of PBAs containing the chlorine group is the optimal sample for assessing the feasibility of the current reaction system. As shown in Table 2, Cl-PBAs were produced with sufficient yields in both cases of reactions of AN and chlorine-substituted BADs (entries 2–4) and reactions of chlorine-substituted ANs and BAD (entries 5 and 6).

4. Conclusions

A one-pot synthesis of *N*-phenylbenzylamine (PBA) from benzaldehyde (BAD) and aniline (AN) was successfully achieved over gold (Au)-loaded carbon nitride (Au–C_3N_4) in the presence of an organic acid. This reaction consisted of two processes and the organic acid fulfilled two functions: (1) as an acid catalyst for the condensation of AN and BAD, producing benzylideneaniline (BAN) in the initial thermal step, and (2) as a hole scavenger (hydrogen source) for the hydrogenation of BAN to PBA in the subsequent photocatalytic step over Au–C_3N_4. Among the organic acids examined, oxalic acid was found to be the most effective due to its capacity to maintain an acidic pH environment as a divalent acid and its ability to effectively capture positive holes as a hole scavenger, resulting in the generation of carbon dioxide. When oxalic acid was used, PBA was obtained with a yield of >99%. A series of experiments revealed that Au–C_3N_4 can be utilized at least three times for the production of halogen-substituted PBA.

Data availability

The data supporting this article have been included as part of the ESI.†

Conflicts of interest

There are no conflicts of interest to declare.

Acknowledgements

This work was partly supported by JSPS KAKENHI Grants 23K17964, 23H01767 and 22H00274 and by a fund from Nippon Sheet Glass Foundation for Materials Science and Engineering. A. T. is grateful for financial support from Japan Petroleum and Carbon Neutral Fuels Energy Center (JPEC).

References

1 R. N. Salvatore, C. H. Yoon and K. W. Jung, *Tetrahedron*, 2001, **57**, 7785–7811.
2 S. A. Lawrence, *Amines: Synthesis Properties and Applications*, Cambridge University Press, Cambridge, 2004.
3 R. F. Borch, M. D. Bernstein and H. D. Durst, *J. Am. Chem. Soc.*, 1971, **93**, 2897–2904.
4 Y. Tsuji, R. Takeuchi, H. Ogawa and Y. Watanabe, *Chem. Lett.*, 1986, 293–294.
5 S. Michlik and R. Kempe, *Chem. – Eur. J.*, 2010, **16**, 13193–13198.
6 A. Bartoszewicz, R. Marcos, S. Sahoo, A. K. Inge, X. Zou and B. Martín-Matute, *Chem. – Eur. J.*, 2012, **18**, 14510–14519.
7 R. Ghalta, A. K. Kar and R. Srivastava, *Chem. – Asian J.*, 2021, **16**, 3790–3803.
8 L.-M. Wang, K. Kobayashi, M. Arisawa, S. Saito and H. Naka, *Org. Lett.*, 2019, **21**, 341–344.
9 G. S. More, N. Kushwaha, R. Bal and R. Srivastava, *J. Colloid Interface Sci.*, 2022, **619**, 14–27.
10 E. Fudo, Y. Kiyota, R. Osawa, A. Tanaka and H. Kominami, *Appl. Catal., A*, 2023, **657**, 119156.
11 G. Dong, Y. Zhang, Q. Pan and J. Qiu, *J. Photochem. Photobiol., C*, 2014, **20**, 33–50.
12 W.-J. Ong, L.-L. Tan, Y. H. Ng, S.-T. Yong and S.-P. Chai, *Chem. Rev.*, 2016, **116**, 7159–7329.
13 L. Jiang, X. Yuan, Y. Pan, J. Liang, G. Zeng, Z. Wu and H. Wang, *Appl. Catal., B*, 2017, **217**, 388–406.
14 Z. Zhou, Y. Zhang, Y. Shen, S. Liu and Y. Zhang, *Chem. Soc. Rev.*, 2018, **47**, 2298–2321.
15 I. F. Teixeira, E. C. M. Barbosa, S. C. E. Tsang and P. H. C. Camargo, *Chem. Soc. Rev.*, 2018, **47**, 7783–7817.
16 A. Kumar, P. Raizada, A. Hosseini-Bandegharaei, V. K. Thakur, V.-H. Nguyen and P. Singh, *J. Mater. Chem. A*, 2021, **9**, 111–153.
17 R. S. Varma, R. Dahiya and S. Kumar, *Tetrahedron Lett.*, 1997, **38**, 2039–2042.
18 G. Liu, D. A. Cogan, T. D. Owens, T. P. Tang and J. A. Ellman, *J. Org. Chem.*, 1999, **64**, 1278–1284.
19 H. Naeimi, F. Salimi and K. Rabiei, *J. Mol. Catal. A: Chem.*, 2006, **260**, 100–104.
20 J. T. Reeves, M. D. Visco, M. A. Marsini, N. Grinberg, C. A. Busacca, A. E. Mattson and C. H. Senanayake, *Org. Lett.*, 2015, **17**, 2442–2445.
21 B. Chen, L. Wang and S. Gao, *ACS Catal.*, 2015, **5**, 5851–5876.

